Reactivity of bis(diphenylphosphines)digold(I) dications with azotate neutral heterocycles: X-ray crystal structure of eclipsed $[\mu\text{-dppmAu}_2(\text{pzH})_2]^{2+}\cdot2\text{ClO}_4^-\cdot\text{H}_2\text{O}$ and staggered $[\mu\text{-dppeAu}_2(\text{pzH})_2]^{2+}\cdot2\text{ClO}_4^-$ complexes

Fiorella Bachechi [a], Alfredo Burini [b,*], Rossana Galassi [b], Bianca Rosa Pietroni [b], Massimiliano Severini [b]

[a] *Istituto di Strutturistica Chimica 'G. Giacomello' CNR, Roma, Italy*
[b] *Dipartimento di Scienze Chimiche Università, via S. Agostino 1, I-62032 Camerino, Italy*

Abstract

Dinuclear gold(I) dicationic complexes were prepared reacting $[\mu\text{-dpp(CH}_2)_n\text{Au}_2]^{2+}$ $(\text{dpp(CH}_2)_n = \text{bis(diphenylphos-phine)alkane}$; $n = 1, 2, 3$) with azotate neutral heterocycles. Using 3,5-dimethylpyrazole (pzH) as ancillary ligand and ClO_4^- as counterion, insoluble polymeric species were obtained by a kinetic control of the reactions; extractions by hot chloroform yield the corresponding monomeric derivatives $[\mu\text{-dpp(CH}_2)_n\text{Au}_2(\text{pzH})_2]^{2+}\cdot2\text{ClO}_4^-$ (**I**, **IIa**, **III**). In one case using NO_3^- instead of ClO_4^- anion the monomeric specie (**IIb**) was directly obtained. Using as neutral coordinating ligand bis(imidazo-2-yl)methane (BIMH$_2$), ten- and 11-membered heterobridged cyclic derivatives $[\mu\text{-dpp(CH}_2)_n\text{Au}_2\mu\text{-BIMH}_2]^{2+}\cdot2\text{ClO}_4^-$ (**IV**, **V**) were also obtained. $^{31}\text{P-NMR}$ spectrum of (**IV**) revealed partial and complete opening of the cycle in solution. The X-ray crystal structures of $[\mu\text{-dppmAu}_2(\text{pzH})_2]^{2+}\cdot2\text{ClO}_4^-\cdot\text{H}_2\text{O}$ (**I**) and $[\mu\text{-dppeAu}_2(\text{pzH})_2]^{2+}\cdot2\text{ClO}_4^-$ (**IIa**) are reported ((**I**): monoclinic, space group $P2_1/n$, $a = 12.253(4)$, $b = 19.417(3)$, $c = 19.152(2)$ Å, $\beta = 97.90(2)°$, $Z = 4$; (**IIa**): monoclinic, space group $P2_1/n$, $a = 10.997(3)$, $b = 13.629(2)$, $c = 14.812(2)$ Å, $\beta = 104.63(1)°$, $Z = 2$). The short intramolecular Au⋯Au distance of 3.133(2) Å found in complex (**I**) indicates a metal–metal interaction. © 1999 Elsevier Science S.A. All rights reserved.

Keywords: Gold; Dinuclear complexes; Bis(diphenylphosphine)alkane; Azoles; Structures

1. Introduction

In the last decade, explosive growth of gold chemistry was observed and, in addition to consolidating its anti-arthritic activity, some gold drugs seem to be effective in the treatment of diseases such as tumors, psoriasis and AIDS [1].

Another characterizing aspect of gold chemistry is the ability of gold atoms to form weak metal–metal interactions, which have been assigned to relativistic effects [2], yielding for example the amazing compound $\{\text{C}[\text{AuP}(\text{C}_6\text{H}_5)_3]_6\}^{2+}$ [3].

In recent years, bis(phosphine)alkanes have been attracting much attention in gold chemistry, mainly because of the ability of these ligands:

1. to stabilize gold(I) complexes
2. to provide dinuclear gold(I) compounds where gold–gold interactions could occur [4]
3. to give homo- or heterobridged cyclic gold(I) derivatives [5]
4. to act as a chelating ligand to gold(I) atoms [6]
5. to yield gold(I) compounds with anti-tumor properties [7].

* Corresponding author. Tel.: + 39-737-402243; fax: + 39-737-637345; e-mail: burini@camserv.unicam.it.

Table 1
^{1}H-, ^{31}P{H}-NMR and other data

| Compound	Yield (%)	Conductivity[a]	Aliphatic protons	Aromatic protons	N–H protons	^{31}P
I	75	140; 11	2.18 (s, 6H); 2.43 (s, 6H); 3.92 (t, 2H); $^2J_{(H-P)} = 13.20$	5.88 (s, 2H); 7.39 (m, 12H); 7.68 (m, 8H)	11.93 (s, 2H)	26.87 (s)
IIa	84	191; 35	2.39 (s, 12H); 2.89 (s, 4H)	6.10 (s, 2H); 7.54 (m, 12 H); 7.76 (m, 8H)	12.30 (s, br, 2H)	29.78 (s)
IIb	81	69; 13	2.39 (s, 12H); 2.99 (s, 4H)	6.06 (s, 2H); 7.50 (m, 12 H); 7.88 (m, 8H)	14.58 (s, br, 2H)	30.64 (s)
III	65	196; 28	2.09 (m, 2H); 2.95 (m, 4H); 2.34 (s, 6H); 2.38 (s, 6H)	6.08 (s, 2H); 7.47 (m, 12H); 7.75 (m, 8H)	12.21 (s, 2H)	27.50 (s)
IV	50	140	3.75 (m, br,2H); 4.65 (m, br, 2H)	7.08 (d, 2H); 7.18 (d, 2 H); 7.38 (m, 12H); 7.62 (m, 8H)	11.98 (s, br, 2H)	29.14 (s), 28.26 (s), 26.91 (s)
V	55	154	3.34 (d, 4H); 4.87 (s, 2H)	7.10 (d, 2H); 7.26 (d, 2H); 7.57 (m, 20H)	12.05 (s, br, 2H)	24.47 (s)

[a] Conductivity was measured in acetone (first number) and dichloromethane (second number) solutions and it is expressed as Ω^{-1} cm^2 mol^{-1}.
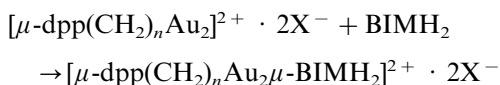
We recently reported the interaction of [μ-bis(phosphine)Au$_2$]$^{2+}$ with 1,3 asymmetric or 1,5 symmetric bihapto ligands yielding heterobridged ring complexes [8]. Now we extend the study to the reactivity of [μ-bis(phosphine)Au$_2$]$^{2+}$ with other azotate heterocycles; our studies could be used as model for interactions of dicationic dinuclear gold(I) complexes in biological systems.

2. Results and discussion

Dinuclear gold(I) dicationic complexes were prepared reacting [μ-dpp(CH$_2$)$_n$Au$_2$]$^{2+}$ (dpp(CH$_2$)$_n$ = bis(diphenylphosphines)alkane) with azotate neutral heterocycles:

[μ-dpp(CH$_2$)$_n$Au$_2$]$^{2+}$ · 2X$^-$ + 2pzH

→ [μ-dpp(CH$_2$)$_n$Au$_2$(pzH)$_2$]$^{2+}$ · 2X$^-$
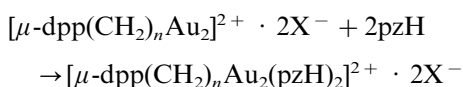
(pzH = 3,5-dimethylpyrazole) [where $n = 1$ and X$^-$ = ClO$_4^-$: (**I**), $n = 2$ and X$^-$ = ClO$_4^-$: (**IIa**), $n = 2$ and X$^-$ = NO$_3^-$: (**IIb**), $n = 3$ and X$^-$ = ClO$_4^-$: (**III**)]

[μ-dpp(CH$_2$)$_n$Au$_2$]$^{2+}$ · 2X$^-$ + BIMH$_2$

→ [μ-dpp(CH$_2$)$_n$Au$_2\mu$-BIMH$_2$]$^{2+}$ · 2X$^-$

(BIMH$_2$ = bis(imidazo-2-yl)methane) [where $n = 1$ and X$^-$ = ClO$_4^-$: (**IV**), $n = 2$ and X$^-$ = ClO$_4^-$: (**V**)]

The use of ClO$_4^-$ as the counterion (**I**, **IIa**, **III**) yielded the formation of relevant amount of products insoluble in THF, and slightly soluble in hot halogenated solvents (CHCl$_3$, CH$_2$Cl$_2$); thus prolonged extractions by chloroform upon warming were necessary to obtain the analytical samples (see experimental part). It is likely that the insoluble products have an oligomeric or polymeric nature due to the ability of the perchlorate anion to form partial or infinite chains by intermolecular hydrogen bonds. The monomeric nature

of the compounds isolated after extraction, matches with their solubilities in most of the common organic solvents and with the molecular structures of complexes (**I**) and (**IIa**). Considering these experimental data we can argue that the oligomeric or polymeric products have been obtained by kinetic control of the reactions, while the monomeric species should be thermodynamically more stable.

Using NO$_3^-$ (**IIb**) instead of ClO$_4^-$ anion we obtained the monomeric soluble compound directly, thus indicating the minor ability of the nitrate anion to form more than one hydrogen bond.

When 2-methylimidazole (ImH) and ClO$_4^-$ were employed, completely insoluble derivatives were obtained. They were a little more stable than the polymeric compounds obtained with a pyrazole ligand and a large amount of decomposed material was obtained upon extraction with hot organic solvents. Low yields of [μ-dpp(CH$_2$)$_n$Au$_2$(ImH)$_2$]$^{2+}$·2X$^-$ with satisfactory elemental analyses were obtained when X = NO$_3$ and $n = 1, 2$.

All the compounds were characterized by elemental analysis, conductivity, IR, ^{1}H- and ^{31}P-NMR spectroscopy. Compounds (**I**), (**IIa**), (**III**) [9] were also characterized by X-ray crystal structure determinations.

Conductivity measures were recorded in acetone and dichloromethane solutions (Table 1). Compounds (**IIa**) and (**III**) behave as 1:2 electrolytes [10], while the stronger coordination of the anion in (**IIb**) is highlighted by a lower conductance value.

Compounds (**I**), (**IV**) and (**V**) show borderline behavior between 1:1 and 2:1 electrolytes underlying a similar trend among open ring and closed compounds [10].

2.1. NMR investigation

The ^{1}H-NMR spectra of the dinuclear gold compounds (**I–III**) (Table 1) show all the signals expected
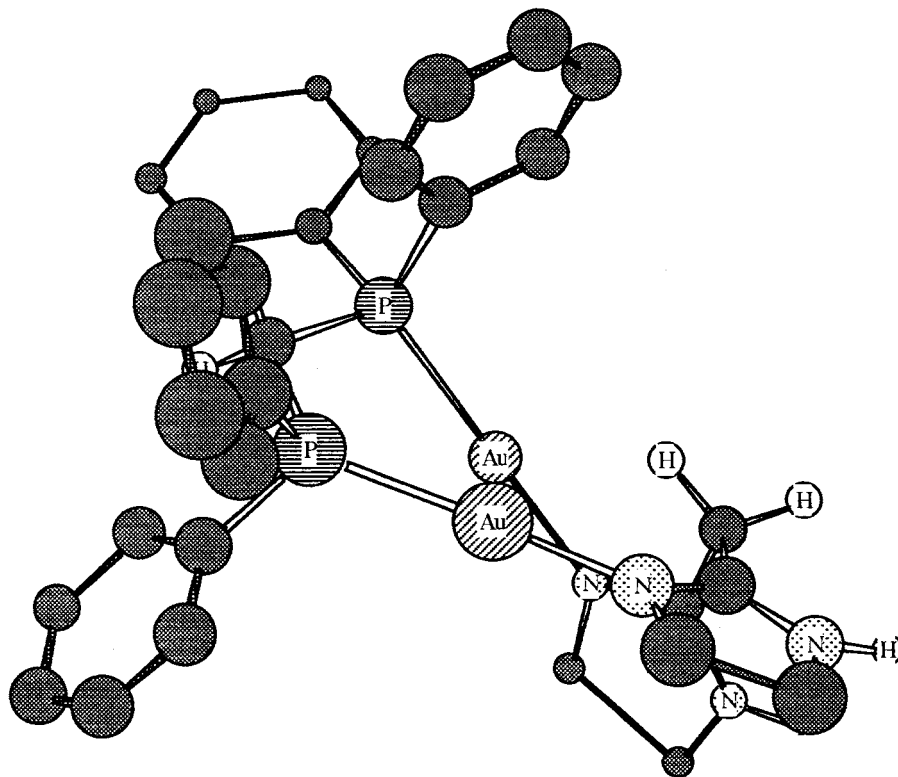
Fig. 1. Molecular model of (**IV**) (ten-membered ring) generated by (CSC Chem3D/Plus). Anions are omitted for clarity.

for the ligands $dpp(CH_2)_n$/pzH in a 1:2 molar ratio; we only found an anomaly in compounds (**IIa,b**). The methyl protons of the pyrazole rings, that we expected to be magnetically not equivalent, resulted to have the same chemical shift at 2.39 ppm. This circumstance could be explained if we suppose that in solution the pyrazole rings are coordinated to the gold atoms by N(1) or N(2) alternatively giving a linkage isomerism that should involve a rapid tautomerism. To confirm this thesis we recorded the ^{1}H-NMR spectrum of compound (**IIa**) at $-50°C$; the methyl signal at 2.39 ppm was split in two peaks of equal intensity at 2.42 and 2.33 ppm, indicating that at low temperature the linkage isomerism is jammed. Similar behaviour was observed in the related [(Ph$_3$P)Au(pzH)]BF$_4$ compound [11].

The ^{31}P-NMR chemical shifts of compounds (**I–III**) (Table 1) are consistent with a phosphorous atom bonded to gold(I) and in trans to an azotate heterocycle [12]. The positions of the resonances of the ^{31}P nucleus were slightly affected by the substitution of the chloride atoms with the pyrazole rings, the maximum upfield Δ chemical shift (3.88 ppm) was found between [dppeAu$_2$Cl$_2$] and compound (**IIa**), while the downfield Δ chemical shift (2.40 ppm) was observed between the starting material [dppmAu$_2$Cl$_2$] and (**I**).

Compounds (**IV**) and (**V**) have the appropriate elemental analyses for a 1:1 molar ratio between the two ligands coordinated to two gold(I) atoms. This is also confirmed by the integrals of the ^{1}H-NMR spectra and conductivity data. By these experimental evidences and considering that gold(I) is usually linearly bicoordinated, we assume that (**IV**) and (**V**) are ten- and 11-membered heterobridged cyclic derivatives (Fig. 1).

The ^{1}H-NMR spectrum of (**IV**) shows two broad multiplets at 3.75 and 4.65 ppm that can be assigned to the methylene groups of the phosphine and BIMH$_2$ ligands respectively. The ^{31}P-NMR of (**IV**), recorded at room temperature (r.t.), shows three singlets at 29.14, 28.26 and 26.91 ppm in a 1:7:2 ratio, respectively. These signals could be attributed to the products generated from a partial and complete opening of the ten-membered cycle of (**IV**), as the signal at 26.91 ppm can be assigned at the ionic specie [μ-dppmAu$_2$]$^{2+}$. This hypothesis was confirmed by the evidence that the pattern remains nearly unchanged even in the ^{31}P-NMR spectrum recorded at 333 K. At this temperature the signal at 26.91 ppm increased, whilst at 193 K only two signals are observed in a 9:1 ratio, most likely due to the closed and partially closed structure of (**IV**), respectively, since the resonance for [dppmAu$_2$]$^{2+}$ disappeared.

The ^{31}P-NMR chemical shifts of compounds (**IV**) and (**V**) decrease as the cycle sizes become bigger. This trend was also observed in analogous compounds previously reported [8] where the azotate bridging ligand is 1,1′-methylenedipyrazole instead of BIMH$_2$.

Table 2
Crystallographic data for (**I**) and (**IIa**)

Compound	(**I**)	(**IIa**)
Empirical formula	$C_{35}H_{38}N_4P_2Au_2Cl_2O_9$	$C_{36}H_{40}N_4P_2Au_2Cl_2O_8$
Formula weight	1185.49	1183.53
Crystal size (mm)	$0.25 \times 0.25 \times 0.40$	$0.3 \times 0.4 \times 0.7$
Crystal system	Monoclinic	Monoclinic
a (Å)	12.253(4)	10.997(3)
b (Å)	19.417(3)	13.629(2)
c (Å)	19.152(2)	14.812(2)
β (°)	97.90(2)	104.63(1)
V (Å^3)	4513(3)	2148(7)
Space group	$P2_1/n(14)$	$P2_1/n(14)$
Z	4	2
$D_{calc.}$ (g cm^{-3})	1.745	1.830
$F(000)$	2280	1140
μ(Cu–K$_\alpha$) (cm^{-1})	144.46	151.57
Diffractometer	Rigaku AFC5R	Rigaku AFC5R
Scan type	$\omega - 2\theta$	$\omega - 2\theta$
Scan rate (° min^{-1})	8.0 (3 rescans)	16.0 (3 rescans)
Scan width (°)	$1.00 + 0.30 \tan \theta$	$1.31 + 0.30 \tan \theta$
2θ max (°)	124.2	123.9
Total measured reflections	7738	3746
Unique reflections	7400 ($R_{int} = 0.059$)	3543 ($R_{int} = 0.063$)
Corrections	Lorentz-polarization absorption	Lorentz-polarization absorption
Transmission factors	0.69–1.00	0.48–1.00
Structure solution	Patterson method	Patterson method
Refinement	Full-matrix least-squares	Full-matrix least-squares
Function minimized	$\Sigma w(\lvert F_o \rvert - \lvert F_o \rvert)^2$	$\Sigma w(\lvert F_o \rvert - \lvert F_o \rvert)^2$
Least-squares weights	$4F_o^2/\sigma^2(F_o^2)$	$4F_o^2/\sigma^2(F_o^2)$
p-factor	0.03	0.03
Anomalous dispersion	All non-hydrogen atoms	All non-hydrogen atoms
Observed reflections	4247 ($I > 5.00\sigma(I)$)	2471 ($I > 3.00\sigma(I)$)
Variables	487	244
Reflections/Parameters	8.72	10.13
R; Rw	0.061; 0.091	0.044; 0.065
Goodness-of-fit	3.36	2.87
Max shift/error	1.72	0.64
Max, min difference peak and hole (e Å^{-3})	1.53, −2.13	1.44, −1.87

2.2. IR spectroscopy

The analyses of IR spectra in the range 4000–300 cm^{-1} confirmed the assumptions made in the previous section.

In compounds (**I**), (**IIa**) and (**III**) bands were found for the weakly coordinating ClO_4^- ligand [13]. The ν_3 absorption at 1087 cm^{-1} and the presence of shoulders at 1070 and 1050 cm^{-1} provide sufficient information about its coordination.

In compound (**IIb**), according to the conductivity value, the NO_3^- anion was found as a strongly coordinated counterion [14], with bands at 818 cm^{-1} (ν_2, weak) and 1040 cm^{-1} (ν_1, medium) only allowed in lower symmetries.

The N–H stretching occurring at lower wavenumber in (**IIb**) (3180 cm^{-1}) than in the perchlorate compound (**IIa**) (3200 cm^{-1}), suggests a stronger N–H coordination in the nitrate than in the perchlorate anion [13].

In cyclic compounds (**IV**) and (**V**) bands at 1087 cm^{-1} (strong and broad) and 620 cm^{-1} (weak) were found revealing ionic ClO_4^- anions. In compounds (**I**–**V**) the presence of medium bands ranging between 352 and 354 cm^{-1} were assigned to Au–P stretching.

3. X-ray structure determination of (I) and (IIa)

3.1. Crystal data

Single crystal measurements for (**I**) and (**IIa**) were made on a Rigaku AFC5R diffractometer with graphite monochromated Cu–K$_\alpha$ radiation and a 12 K/V rotating anods generator. The data were collected using the $\omega - 2\theta$ technique to a maximum 2θ value of 124°. The structures were solved by Patterson and subsequent Fourier syntheses and refined by full-matrix least-squares method with anisotropic thermal parameters
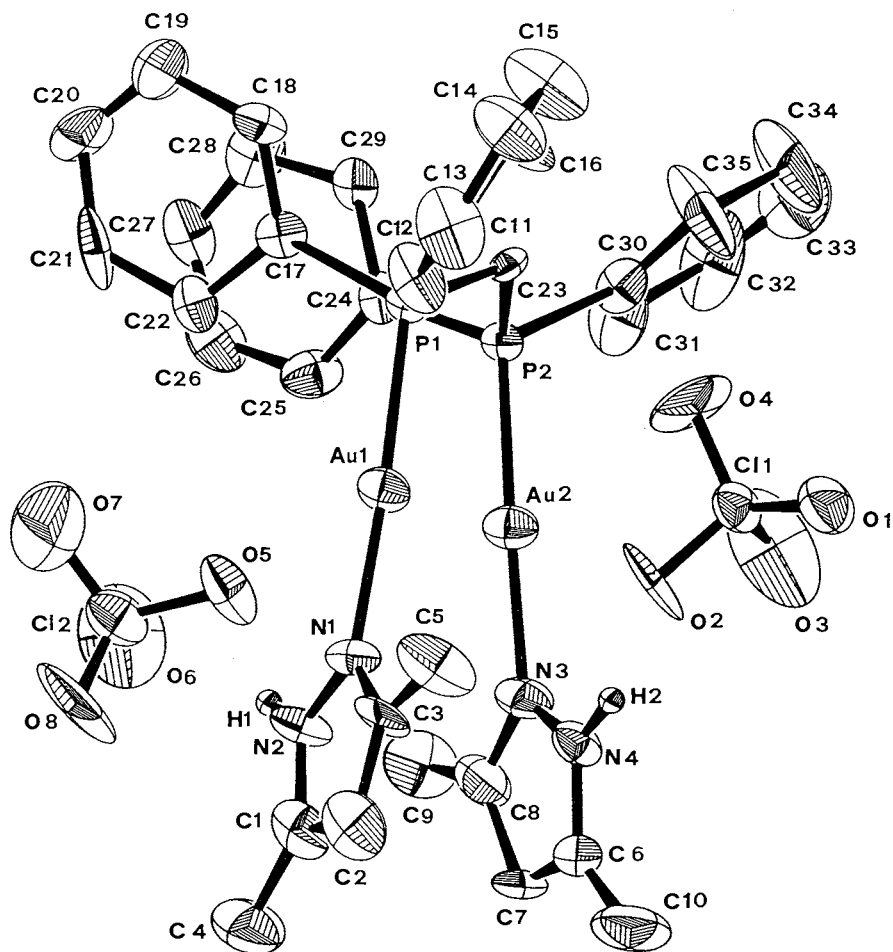
Fig. 2. ORTEP plot of compound (**I**) and the numbering scheme of the atoms.

for all non-hydrogen atoms. The hydrogen atoms were included at calculated positions and not refined. Crystal data and structure determination parameters are given in Table 2. Atomic scattering factor and anomalous dispersion terms were taken from the X-ray crystallographic tables in Ref. [15]. All calculations where performed using the TEXSAN crystallographic software package [16]. One molecule of water was found present in compound (**I**). In compound (**IIa**) the asymmetric unit contains half of the binuclear cationic complex with the connected counterion, the other half and the other counterion being related by a centre of symmetry.

3.2. Description of the structures

The molecular structure of [dppmAu$_2$(3,5-MepzH)$_2$]$^{2+}$ · 2ClO$_4^-$ (**I**) is represented in the ORTEP plot of Fig. 2 together with the numbering scheme; final atomic coordinates are listed in Table 3, while bond distances and angles are listed in Table 4.

The structure of complex (**I**) consists of discrete units where the Au(I) atoms are two-coordinate. The Au–N and Au–P bond lengths are 2.06(2) and 2.234(5) Å for

Au(1), 2.06(2) and 2.231(5) Å for Au(2), respectively, close to those found in [Au$_2$(μ-HX)(μ-dmpe)] (H$_3$X = xanthine; dmpe = 1,2-bis(dimethylphosphine)ethane) ([12]b).

It is interesting to compare the X-ray crystal structure of [dppmAu$_2$Cl$_2$] [17] with that of complex (**I**); while the former shows a staggered conformation, very close to that found in the structure of the free ligand [18], the latter assumes an eclipsed conformation.

Molecular mechanics calculations on related [Au$_2$(dppm)(SR)$_2$] complex have established an energy barrier of 9 kcal mol^{-1} between staggered and eclipsed conformations [19]. It should be pointed out that a reorientation of the phosphine gold complex occurs when the chloride atoms are substituted with pyrazole ligands.

The driving force of this reorientation could be attributed to three kinds of attractive intramolecular interactions cooperating in the molecule of (**I**):

1. between two staking phenyl groups, bound to different phosphorous atoms. The planes of the phenyl groups lie ca. 3.8 Å apart
2. between the gold atoms

3. between the pyrazole rings facing each other at distances from 3.3 to 3.6 Å for the parts which overlap. The N–H groups are oriented in opposite

Table 3
Atomic coordinates and equivalent isotropic thermal parameters of complex (**I**), with estimated S.D. in parentheses

	x/a	y/b	z/c	B_{eq}
Au(1)	0.02117(7)	0.07115(4)	0.87293(4)	3.44(4)
Au(2)	0.01330(7)	0.05306(4)	0.70976(4)	3.59(4)
P(1)	−0.0779(4)	0.1675(2)	0.8533(2)	2.2(2)
P(2)	−0.1107(4)	0.1378(2)	0.6945(2)	2.2(2)
N(1)	0.111(1)	−0.0165(7)	0.9014(8)	3.5(8)
N(2)	0.081(1)	−0.0797(8)	0.8774(8)	3.5(8)
N(3)	0.130(1)	−0.0235(8)	0.7212(8)	3.8(8)
N(4)	0.232(1)	−0.0150(8)	0.7536(8)	3.3(8)
C(1)	0.156(3)	−0.125(1)	0.898(1)	5(1)
C(2)	0.242(2)	−0.088(1)	0.942(1)	6(1)
C(3)	0.209(2)	−0.021(1)	0.944(1)	4(1)
C(4)	0.148(2)	−0.200(1)	0.883(1)	7(1)
C(5)	0.265(2)	0.039(1)	0.983(1)	6(1)
C(6)	0.295(2)	−0.071(1)	0.754(1)	4(1)
C(7)	0.226(2)	−0.120(1)	0.717(1)	6(1)
C(8)	0.118(2)	−0.089(1)	0.698(1)	5(1)
C(9)	0.014(2)	−0.120(1)	0.656(1)	7(1)
C(10)	0.411(2)	−0.077(1)	0.785(1)	7(1)
C(11)	−0.026(2)	0.238(1)	0.908(1)	3(1)
C(12)	0.028(2)	0.224(1)	0.977(1)	5(1)
C(13)	0.068(2)	0.276(1)	1.018(1)	6(2)
C(14)	0.049(2)	0.344(1)	0.999(1)	6(1)
C(15)	0.000(2)	0.360(1)	0.934(1)	7(1)
C(16)	−0.039(2)	0.306(1)	0.890(1)	6(1)
C(17)	−0.220(2)	0.155(1)	0.8660(8)	2.7(8)
C(18)	−0.290(2)	0.207(1)	0.879(1)	4(1)
C(19)	−0.402(2)	0.197(1)	0.887(1)	6(1)
C(20)	−0.439(2)	0.132(2)	0.885(1)	5(1)
C(21)	−0.374(2)	0.076(1)	0.871(1)	5(1)
C(22)	−0.262(2)	0.085(1)	0.863(1)	3(1)
C(23)	−0.086(1)	0.2007(8)	0.7643(8)	2.1(7)
C(24)	−0.250(1)	0.109(1)	0.6918(8)	2.6(8)
C(25)	−0.277(2)	0.040(1)	0.685(1)	4(1)
C(26)	−0.385(2)	0.018(1)	0.681(1)	5(1)
C(27)	−0.466(2)	0.062(1)	0.685(1)	5(1)
C(28)	−0.443(2)	0.131(1)	0.693(1)	5(1)
C(29)	−0.334(2)	0.156(1)	0.6944(8)	3.1(9)
C(30)	−0.107(2)	0.188(1)	0.6137(9)	4(1)
C(31)	−0.153(2)	0.152(1)	0.548(1)	7(1)
C(32)	−0.155(3)	0.197(2)	0.487(1)	9(2)
C(33)	−0.115(3)	0.261(2)	0.487(2)	8(2)
C(34)	−0.092(3)	0.291(2)	0.540(2)	10(2)
C(35)	−0.078(3)	0.256(1)	0.614(2)	10(2)
Cl(1)	0.2637(5)	0.1738(3)	0.7777(3)	3.7(3)
O(1)	0.355(1)	0.2153(8)	0.7916(8)	5.7(9)
O(2)	0.268(1)	0.117(1)	0.819(1)	8(1)
O(3)	0.263(2)	0.148(1)	0.715(1)	12(2)
O(4)	0.173(2)	0.210(1)	0.786(1)	12(2)
Cl(2)	−0.2071(6)	−0.1207(3)	0.8071(4)	4.9(3)
O(5)	−0.134(1)	−0.0663(8)	0.7949(8)	5.9(8)
O(6)	−0.249(2)	−0.148(1)	0.744(1)	11(1)
O(7)	−0.300(2)	−0.096(1)	0.830(1)	13(2)
O(8)	−0.156(2)	−0.165(1)	0.853(1)	11(2)
O(9)	0.726(2)	−0.011(1)	0.451(1)	13(2)

Table 4
Selected bond distances (Å) and angles (°) of complex (**I**)

Bond length (Å)

Au(1)···Au(2)	3.133(1)	N(2)–C(1)	1.30(3)
Au(1)–P(1)	2.234(5)	N(3)–N(4)	1.32(2)
Au(1)–N(1)	2.06(1)	N(3)–C(8)	1.35(3)
Au(2)–P(2)	2.231(5)	N(4)–C(6)	1.33(2)
Au(2)–N(3)	2.06(2)	C(1)–C(2)	1.45(3)
P(1)–C(11)	1.79(2)	C(1)–C(4)	1.48(3)
P(1)–C(17)	1.81(2)	C(2)–C(3)	1.36(3)
P(1)–C(23)	1.81(2)	C(3)–C(5)	1.50(3)
P(2)–C(23)	1.81(2)	C(6)–C(7)	1.40(3)
P(2)–C(24)	1.79(2)	C(6)–C(10)	1.47(3)
P(2)–C(30)	1.84(2)	C(7)–C(8)	1.46(3)
N(1)–N(2)	1.34(2)	C(8)–C(9)	1.53(3)
N(1)–C(3)	1.36(2)		

Bond angle (°)

Au(2)···Au(1)–P(1)	89.1(1)	N(3)–N(4)–C(6)	114(2)
Au(2)···Au(1)–N(1)	96.5(4)	N(2)–C(1)–C(2)	105(2)
Au(1)···Au(2)–P(2)	88.5(1)	N(2)–C(1)–C(4)	125(3)
Au(1)···Au(2)–N(3)	92.8(4)	C(2)–C(1)–C(4)	129(3)
P(1)–Au(1)–N(1)	174.3(4)	C(1)–C(2)–C(3)	108(2)
P(2)–Au(2)–N(3)	178.0(5)	N(1)–C(3)–C(2)	106(2)
Au(1)–P(1)–C(11)	113.9(7)	N(1)–C(3)–C(5)	124(2)
Au(1)–P(1)–C(17)	112.2(6)	C(2)–C(3)–C(5)	130(2)
Au(1)–P(1)–C(23)	114.4(5)	N(4)–C(6)–C(7)	104(2)
C(11)–P(1)–C(17)	107.1(9)	N(4)–C(6)–C(10)	126(2)
C(11)–P(1)–C(23)	104.2(8)	C(7)–C(6)–C(10)	130(2)
C(17)–P(1)–C(23)	104.2(7)	C(6)–C(7)–C(8)	108(2)
Au(2)–P(2)–C(23)	111.1(5)	N(3)–C(8)–C(7)	105(2)
Au(2)–P(2)–C(24)	113.6(7)	N(3)–C(8)–C(9)	126(2)
Au(2)–P(2)–C(30)	114.0(6)	C(7)–C(8)–C(9)	129(2)
C(23)–P(2)–C(24)	107.4(8)	P(1)–C(11)–C(12)	118(2)
C(23)–P(2)–C(30)	104.0(9)	P(1)–C(11)–C(16)	125(2)
C(24)–P(2)–C(30)	106.1(9)	P(1)–C(17)–C(18)	125(2)
Au(1)–N(1)–N(2)	123(1)	P(1)–C(17)–C(22)	117(1)
Au(1)–N(1)–C(3)	127(1)	P(1)–C(23)–P(2)	115.9(9)
N(2)–N(1)–C(3)	109(2)	P(2)–C(24)–C(25)	122(2)
N(1)–N(2)–C(1)	111(2)	P(2)–C(24)–C(29)	120(1)
Au(2)–N(3)–N(4)	124(1)	P(2)–C(30)–C(31)	114(2)
Au(2)–N(3)–C(8)	127(2)	P(2)–C(30)–C(35)	124(2)
N(4)–N(3)–C(8)	109(2)		

direction to reduce the steric hindrance of the methyl groups.

All the attractive intramolecular interactions result in the formation of a molecular zipper leading to an eclipsed conformation with a torsion angle Au–P–P–Au of 9.4(2)°, hence compound (**I**) can be classified as an open ring complex.

The Au1···Au2 distance of 3.133(1) Å, is indicative of a d^{10}–d^{10} closed shell metal interaction. The gold–gold distance found in (**I**) is shorter than that observed in [dppmAu$_2$Cl$_2$] (3.351(2) Å) and slightly longer than that one found in [syn/syn(CH$_3$)$_3$P=C(P(Ph)$_2$)$_2$Au$_2$Cl$_2$] (3.000(1)Å) [20].

The P–Au–N angles of 174.3(4) and 178.0 (5)° with a deviation from linearity are further evidence of the gold–gold attraction. The two perchlorato anions are bound, by hydrogen bonding, to the heterocycles.
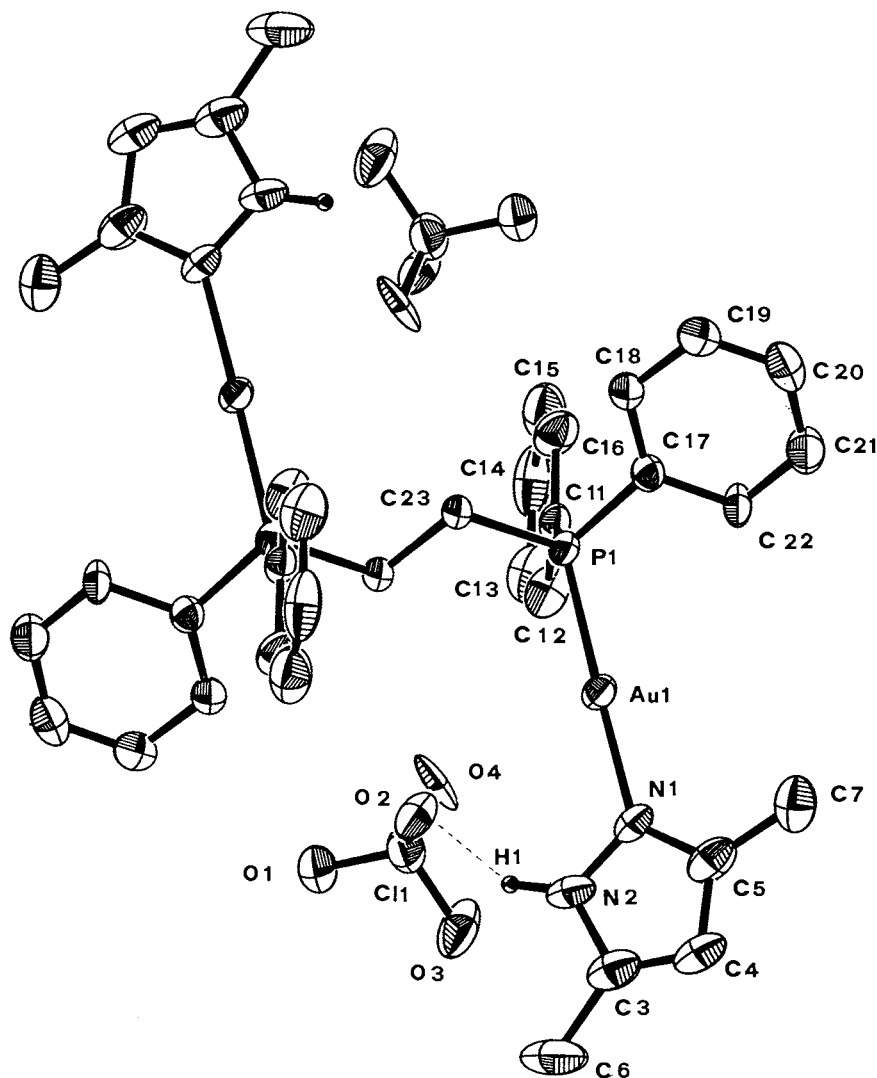
Fig. 3. ORTEP plot of compound (**IIa**) and the numbering scheme of the atoms.

The molecular structure of complex [dppeAu$_2$(3,5-MepzH)$_2$]$^{2+}$·2ClO$_4^-$ (**IIa**) is represented in the ORTEP plot of Fig. 3 together with the numbering scheme; final atomic coordinates are listed in Table 5, and bond distances and angles are listed in Table 6.

The structure of compound (**IIa**) is centrosymmetric; therefore the linear coordination units of gold(I) atoms lie on the molecular plane with opposite orientation, resulting in a staggered conformation with a torsional angle Au–P–P–Au of 180°. Also the [dppeAu$_2$Cl$_2$] structure [21] shows a staggered conformation but in this case the torsional angle Au–P–P–Au is 96°.

P–Au (2.232(3) Å) and Au–N distances of 2.060(9) Å are close to those found in neutral complexes ([12]b) indicating that a neutral or negative nitrogen atom may bond to gold with the same strength. The P–Au–N angle of 177.9(3)° is rather different with respect to the P–Au–Cl angle found in [dppeAu$_2$Cl$_2$] (175.4(2)°) where, on the contrary to (**IIa**), intermolecular Au···Au

interactions occur. The absence of such interactions in (**IIa**) could be attributed to an higher steric hindrance of the pyrazole groups compared to the chloride atoms. The absence of intramolecular metal–metal interactions in compound (**IIa**), which in contrast are present in the analogous compound (**I**), could be due to the dppe bridging ligand that forces the gold atoms too far away to interact in eclipsed conformation. Also in complex (**IIa**) the perchlorate anions are bonded to the pyrazole rings by hydrogen bonds.

An intriguing aspect of the above reported structures is the torsion angle Au–P–P–Au, which is 9.4(2) and 180° for (**I**) and (**IIa**), respectively. Comparing these values with those reported for related [μ-dpp(CH$_2$)$_n$Au$_2$Cl$_2$] compounds ($n = 1$, $\theta = 67.5°$; $n = 2$, $\theta = 96°$), it is evident that substitution of chloride atoms with pyrazole ligands causes a drastic change in torsional angles ($n = 1$, $\Delta_q = -56.1°$; $n = 2$, $\Delta_q = +84°$). We observed that this behavior might be corre-

Table 5
Atomic coordinates and equivalent isotropic thermal parameters of complex (**IIa**), with estimated S.D. in parentheses

	x/a	y/b	z/c	B_{eq}
Au(1)	0.74810(4)	0.46411(3)	0.59912(3)	4.66(3)
P(1)	0.9163(2)	0.5595(2)	0.6102(2)	4.2(1)
N(1)	0.5887(8)	0.3803t7)	0.5866(6)	5.5(4)
N(2)	0.5886(8)	0.2841(8)	0.5592(7)	6.2(5)
C(3)	0.482(1)	0.240(1)	0.566(1)	7.7(7)
C(4)	0.416(1)	0.307(1)	0.598(1)	8.2(8)
C(5)	0.482(1)	0.397(1)	0.6101(9)	7.0(6)
C(6)	0.466(2)	0.131(1)	0.544(1)	11(1)
C(7)	0.453(1)	0.495(1)	0.645(1)	8.6(8)
C(11)	1.049(1)	0.5288(7)	0.7046(7)	4.8(5)
C(12)	1.057(1)	0.440(1)	0.750(1)	7.3(7)
C(13)	1.159(2)	0.413(1)	0.816(1)	9.0(9)
C(14)	1.257(2)	0.481(2)	0.844(1)	10(1)
C(15)	1.251(1)	0.572(2)	0.804(1)	9.3(9)
C(16)	1.148(1)	0.594(1)	0.735(1)	7.3(6)
C(17)	0.876(1)	0.6866(7)	0.6245(6)	4.6(4)
C(18)	0.923(1)	0.7627(8)	0.5848(8)	5.6(5)
C(19)	0.887(1)	0.8587(9)	0.6017(9)	6.4(6)
C(20)	0.807(1)	0.873(1)	0.655(1)	7.3(7)
C(21)	0.761(1)	0.796(1)	0.6948(9)	7.0(7)
C(22)	0.794(1)	0.7027(8)	0.6796(7)	5.5(5)
C(23)	0.979(1)	0.5553(7)	0.5064(7)	4.8(4)
Cl(1)	0.3849(3)	0.3306(2)	0.0975(2)	7.2(2)
O(1)	0.4521(9)	0.4009(6)	0.0620(7)	7.8(5)
O(2)	0.327(1)	0.2607(7)	0.031(1)	7.8(6)
O(3)	0.288(2)	0.375(1)	0.130(1)	10.5(8)
O(4)	0.469(2)	0.282(2)	0.170(2)	12(1)

lated to the relative ^{31}P-NMR Δ chemical shifts [$n = 1$, $\Delta_d = 2.40$ (downfield); $n = 2$, $\Delta_d = 3.88$ (upfield)], even though this data correlation can be argued only considering configuration restraints of (**I**) and (**IIa**) in solution.

Table 6
Selected bond distances (Å) and angles (°) of complex (**IIa**)

Bond length (Å)			
Au(1)–P(1)	2.232(3)	N(2)–C(3)	1.34(1)
Au(1)–N(1)	2.060(9)	C(3)–C(4)	1.33(2)
P(1)–C(11)	1.80(1)	C(3)–C(6)	1.53(2)
P(1)–C(17)	1.81(1)	C(4)–C(5)	1.40(2)
P(1)–C(23)	1.84(1)	C(5)–C(7)	1.50(2)
N(1)–N(2)	1.37(1)	C(11)–C(12)	1.38(2)
N(1)–C(5)	1.33(1)	C(23)–C(23)	1.60(2)

Bond angle (°)			
P(1)–Au(1)–N(1)	177.9(3)	N(2)–C(3)–C(6)	119(2)
Au(1)–P(1)–C(11)	114.6(3)	C(4)–C(3)–C(6)	135(1)
Au(1)–P(1)–C(17)	110.0(3)	C(3)–C(4)–C(5)	109(1)
Au(1)–P(1)–C(23)	113.5(3)	N(1)–C(5)–C(4)	107(1)
C(11)–P(1)–C(17)	107.8(4)	N(1)–C(5)–C(7)	121(1)
C(11)–P(1)–C(23)	104.1(5)	C(4)–C(5)–C(7)	132(1)
C(17)–P(1)–C(23)	106.3(4)	P(1)–C(11)–C(12)	121.8(9)
Au(1)–N(1)–N(2)	119.6(7)	P(1)–C(11)–C(16)	121.4(9)
Au(1)–N(1)–C(5)	132.4(9)	P(1)–C(17)–C(18)	123.3(7)
N(2)–N(1)–C(5)	108(1)	P(1)–C(17)–C(22)	115.9(8)
N(1)–N(2)–C(3)	110(1)	P(1)–C(23)–C(23)	108.0(8)
N(2)–C(3)–C(4)	107(1)		

4. Experimental

Elemental analyses were carried out by Carlo Erba 1106 elemental microanalyzer. ^{1}H- and ^{31}P{H}-NMR spectra were recorded in deuterated chloroform solution on Varian VXR-300 instrument at 300 MHz or on a Varian Gemini 200 instrument at 200 MHz, using SiMe$_4$ or 85% H$_3$PO$_4$ as the internal standard. Chemical shifts are reported as δ in units of parts per million (ppm), while coupling constants are reported in hertz (Hz). The following abbreviations were employed: s, singlet; d, doublet; t, triplet; m, multiplet; br, broad. Infrared spectra were recorded in the range 4000–200 cm^{-1} on a Perkin-Elmer 1310 spectrophotometer using Nujol mulls in sodium chloride or polyethylene windows. Conductivities were measured at 25°C on Crison conductimeter 522 using 1×10^{-3} M acetone and dichloromethane solutions. A dinitrogen atmosphere was always used; moreover the products were obtained carrying out the reactions in darkness. THF was purified by conventional methods prior to use.

Compounds (**I–V**) have satisfactory elemental analyses. [dppmAu$_2$Cl$_2$] [22], [dppeAu$_2$Cl$_2$] [23], [dpppAu$_2$Cl$_2$] [24], and bis(imidazo-2-yl)methane (BIMH$_2$) [25] were prepared as described.

4.1. Synthesis of [dppmAu$_2$ (3,5-MepzH)$_2$]$^{2+}$ · 2ClO$_4^-$ (I)

To a suspension of [dppmAu$_2$Cl$_2$] (0.352 g, 4.1 × 10^{-1} mmol) in THF (8 ml), AgClO$_4$·H$_2$O (0.1870 g, 8.3 × 10^{-1} mmol) was added. After 30 min, the suspension containing AgCl was transferred by cannula over a Celite bed (ca. 2 cm). The filtered solution was collected in the reaction vessel and the solid 3,5-dimethyl-pyrazole (0.080 g, 8.3 × 10^{-1} mmol) was added. Immediately, a light gray precipitate was formed, and after 3 h the reaction mixture was centrifuged. The precipitate was extracted by hot CHCl$_3$. The chloroform solution was concentrated to give the analytical sample (**I**) (0.278 g). Further product was obtained evaporating the supernatant to dryness; the residue obtained was crystallized by CH$_2$Cl$_2$/hexane to give crystals of (**I**) (0.085 g).

Compounds **IIa**, **IIb**, and **III** were synthesized in a similar way using the appropriate starting materials.

4.2. Synthesis of [dppmAu$_2$(bis(imidazol-2-yl)-methane)]$^{2+}$ · 2ClO$_4^-$ (IV)

To a suspension of [dppmAu$_2$Cl$_2$] (0.230 g, 0.27 mmol) in THF/MeOH (11/6 ml), AgClO$_4$·H$_2$O (0.112 g, 0.27 mmol) and, after 15 min of stirring at r.t., the solid bis(imidazol-2-yl)methane (0.040 g, 0.27 mmol) were